Supporting Information

Baker et al. 10.1073/pnas.1213127109

SI Full Synthetic Procedures

All reagents and solvents were purchased from commercial sources and used without further purification. Complexes were prepared in Erlenmeyer Teflon flasks.

Minor Variation to Increase Yield of 4 (Note That Changes Are to Reaction Time and Chromatography). Pivalic acid (25 g, 245 mmol), di-*iso*propylamine (0.35 g, 3.5 mmol), and chromium(III) fluoride tetrahydrate (5.0 g, 27.6 mmol) were stirred together at 150 °C for 41 h. The flask was cooled to room temperature, MeCN (100 mL) was added, and the solution was stirred for 3 h to produce a solid precipitate. This was collected by filtration and washed with MeCN, and the solid was extracted with acetone (550 mL) while stirring overnight. The resulting solution was filtered and then evaporated to dryness under reduced pressure. The residue contained a mixture of compounds **2**, **3**, and **4**; separation was achieved with column chromatography on silica gel.

With toluene as an eluent, compound **2** elutes first as an intense green band [yield 1.1 g (15%) found after evaporation]. The eluent was changed to 40:1 toluene:ethyl acetate, and **3** was eluted as the next band. Evaporation of the solution under reduced pressure gives **3** as a green powder with a yield of 0.2 g (2.5%). Calculated elemental analysis (%) of **3** as $C_{96}H_{178}Cr_9F_{10}N_1O_{36}$ are Cr 18.14, C 44.68, H 6.95, and N 0.54 compared with experimental values, which gave (%) Cr 18.42, C 44.45, H 7.00, and N 0.45. Positive ion electrospray mass spectrometry (+ES-MS) using THF as carrier solvent gave *m/z* values of +2603 assigned as the molecular ion plus one sodium, $[M + Na]^+$, +2682 assigned $[M + {}^{i}Pr_2NH_2]^+$.

Thereafter a mixture of toluene:ethyl acetate starting with a 20/1 ratio and finishing with a 10/1 ratio was used to elute **4**. After evaporation to dryness, **4** remained as a green powder with a yield of 3.05 g (40%). Calculated elemental analysis (%) of **4** as $C_{91}H_{169}Cr_9F_{11}N_1O_{34}$ are Cr 18.73, C 43.75, H 6.82, and N 0.56 compared to experimental values, which gave (%) Cr 18.58, C 43.30, H 6.79, and N 0.54. Positive ion electrospray mass spectrometry (+ES-MS) using THF as carrier solvent gave *m/z* values of +2520 assigned as the molecular ion plus one sodium, $[M + Na]^+$, +2600 assigned $[M + {}^{i}Pr_2NH_2]^+$.

SI Mass Spectroscopy of Reaction

The monitored reaction used Teflon flasks and was performed at 140 °C. The reagents used were $CrF_3{\cdot}4\ H_2O$ (3.0 g), pivalic acid (20.0 g), and di-*iso*propylamine (0.21 g). After 24 h, further pivalic acid (10 g) was added.

SI Magnetic Data and INS Measurements

Magnetic susceptibility measurements were performed in the temperature range of 1.8–300 K, using a Quantum Design MPMS-XL SQUID magnetometer equipped with a 7-T magnet in a field of 0.5 T. Magnetization measurements were performed at 2 and 4 K using the same equipment. Diamagnetic corrections were estimated using Pascal's constants, and magnetic measurements were corrected for sample holder contributions.

INS was performed on the IN5b time-of-flight inelastic spectrometer (1) at the Institute Laue-Langevin, Grenoble, France, and IRIS at ISIS Science and Technology Facilities Council, Rutherford Appleton Laboratory, United Kingdom, on polycrystalline nondeuterated samples of **3** or **4** loaded into a hollow aluminum cylinder for measurement. The presence of incoherent hydrogen scattering was observed, with magnetic features lying on a broad phonon intensity that increased with wave vector transfer and temperature. A background contribution was added to the simulations to account for phonon intensity contributions. INS energy spectra were obtained by integration of scattering intensity over all detector angles. Detector efficiencies were normalized to a standard vanadium measurement.

SI Modelling of INS and Magnetisation Experimental Data

The simulated INS spectra for **3** and **4**, with the parameters of Table 1, were made by use of effective subspaces of dimension 64 by 64 and 54 by 54, for 3 and 4, respectively, created by diagonalisation of the full spin-Hamiltonian of the system by use of self-written software (2) that makes use of the Davidson algorithm. The magnetisation vs. field of **3** and **4** at 2 and 4 K was also calculated by numerical diagonlisation of the full anisotropic spin-Hamiltonian of the system (square matrix of dimension 262.144), along the X- and Z-axis, by use of our developed sparse matrix approach (2).

SI Density Functional Calculations

The DFT calculations were performed using Noodleman's broken symmetry (BS) approach (3) to compute *J* values. The calculations were performed using Gaussian 09 software (4) using the hybrid B3LYP functional (2, 5, 6). We used a triple zeta valence (7) basis set on Cr and SVP for the rest of the elements (8). Calculations were performed on models of **3** and **4**, where the pivalates were modeled as acetates to reduce the computational time; previous work suggests this is a valid modeling strategy to obtain exchange interactions in relevant polymetallic complexes (9–12). The magnetic exchange interactions were extracted using the pairwise interaction model (12). Energies of five spin configurations were calculated for both **3** and **4.** The five spin configurations calculated were as follows: (*i*) all spin up ($S = 27/2$), (*ii*) spin down on Cr 4, 6, and 8 ($S = 9/2$), (*iii*) spin down on Cr 1 and 9 ($S = 15/2$), (*iv*) spin down on Cr 1 ($S = 21/2$), (*v*) spin down on Cr 5 ($S = 21/2$), and (*vi*) spin down on Cr 3 ($S = 21/2$). (Cr sites are numbered clockwise in Fig. 1*B* with the site with the Y ligand attached as Cr1). The energy difference between the spin configurations are equated to the corresponding exchange interactions from which all three *J* values were extracted. Errors on the computed interactions have been estimated and are included in Table 1 (13).

To estimate the change induced by removal of a single carboxylate group calculations were performed on dimetallic fragments (Fig. S6); the difference in the exchange interaction calculated was around 0.7 meV, similar to that observed between J_{19} and J_{23}.

1. Barone V, Bencini A, Ciofini I, Daul CA, Totti F (1998) Density functional modeling of double exchange interactions in transition metal complexes. Calculation of the ground and excited state properties of $[Fe_2(OH)_3(tmtacn)_2]^{2+}$. *J Am Chem Soc* 120(33): 8357–8365.
2. Piligkos S, et al. (2009) EPR spectroscopy of a family of Cr(III) 7M(II) (M = Cd, Zn, Mn, Ni) "wheels": Studies of isostructural compounds with different spin ground states. *Chem Eur J* 15(13):3152–3167.
3. Sheldrick GM (2008) A short history of SHELX. *Acta Crystallogr A* 64(Pt 1):112–122.
4. Ollivier J, Mutka H (2011) IN5 cold neutron time-of-flight spectrometer, prepared to tackle single crystal spectroscopy. *J Phys Soc Jpn* 80:SB003–SB006.
5. Davidson ER (1975) The iterative calculation of a few of the lowest eigenvalues and corresponding eigenvectors of large real-symmetric matrices. *J Comput Phys* 17(1):87–94.
6. Noodleman L (1981) Valence bond description of anti-ferromagnetic coupling in transition-metal dimers. *J Chem Phys* 74(10):5737–5743.
7. Frisch MJ, et al. (2003) *Gaussian 03, Revision C.01* (Gaussian, Inc., Wallingford, CT).
8. Becke AD (1993) Density-functional thermochemistry.3. The role of exact exchange. *J Chem Phys* 98(7):5648–5652.
9. Ruiz E, Rodríguez-Fortea A, Cano J, Alvarez S, Alemany P (2003) About the calculation of exchange coupling constants in polynuclear transition metal complexes. *J Comput Chem* 24(8):982–989.

10. Ruiz E, Alvarez S, Cano J, Polo V (2005) About the calculation of exchange coupling constants using density-functional theory: The role of the self-interaction error. *J Chem Phys* 123(16):164110.
11. Schaefer A, Huber C, Ahlrichs R (1994) Fully optimized contracted Gaussian-basis sets of triple zeta valence quality for atoms Li to Kr. *J Chem Phys* 100(8):5829–5835.
12. Frisch MJ, Pople JA, Binkley JS (1984) Self-consistent molecular-orbital methods 25. Supplementary functions for Gaussian-basis sets. *J Chem Phys* 80(7):3265–3269.
13. Rajeshkumar T, Rajaraman G (2012) Is a radical bridge a route to strong exchange interactions in lanthanide complexes? A computational examination. *Chem Commun (Camb)* 48(63):7856–7858.

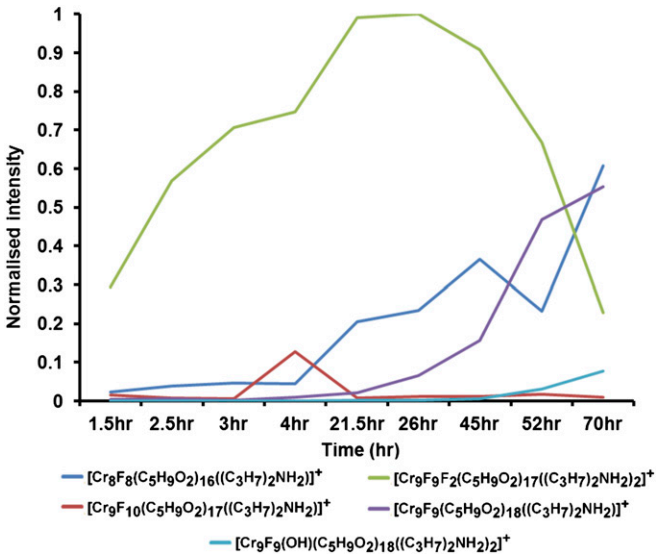

Fig. S1. Intensity of individual components of reaction mixture by cryospray mass spectrometry of the reaction at times indicated.

Reaction Time 25 m.

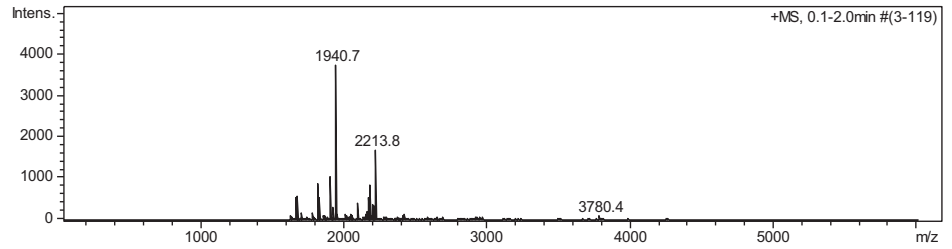

Reaction time: 90 m.

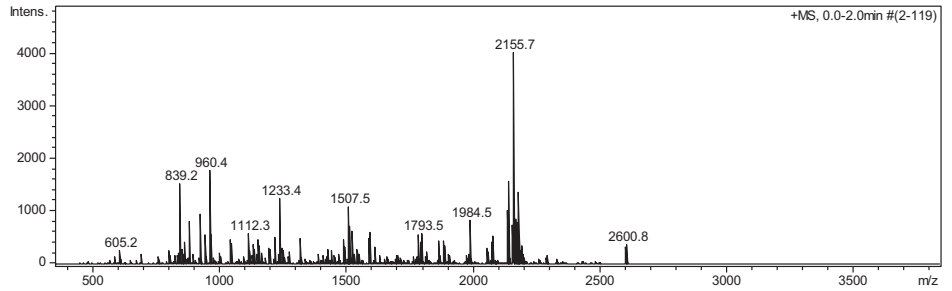

Reaction time 150 m.

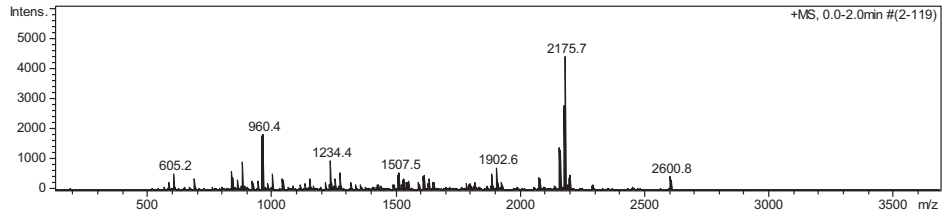

Reaction time: 180 m.

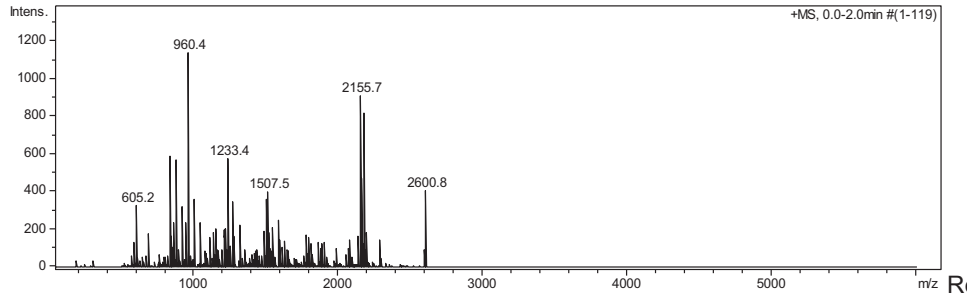

Reaction time: 240 m.

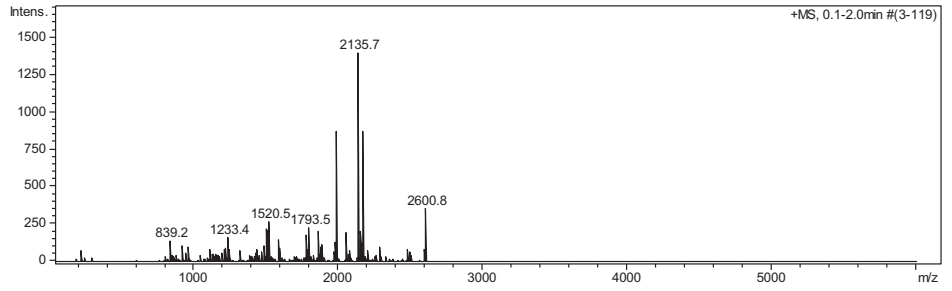

Fig. S2. (Continued)

Reaction time: 21.5 h.

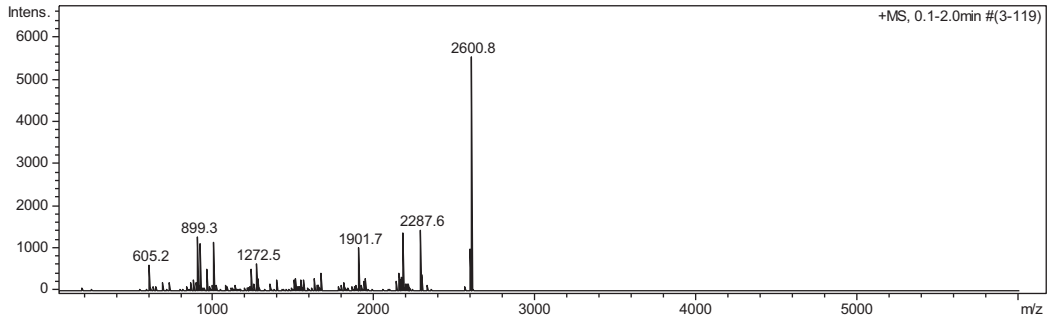

Reaction time: 26 h.

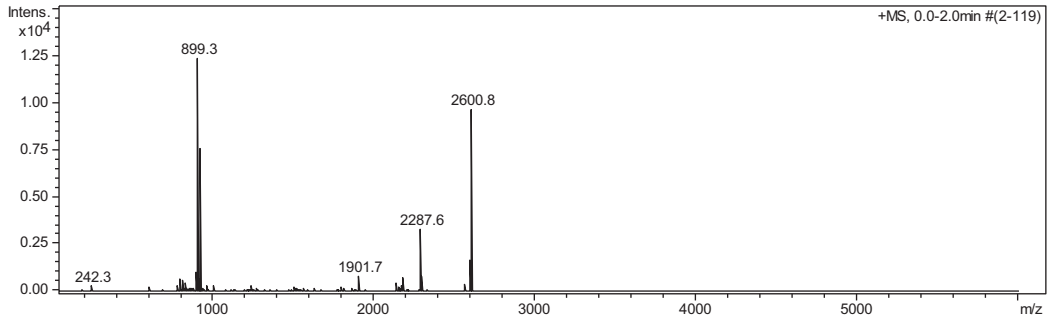

Reaction time: 52 h.

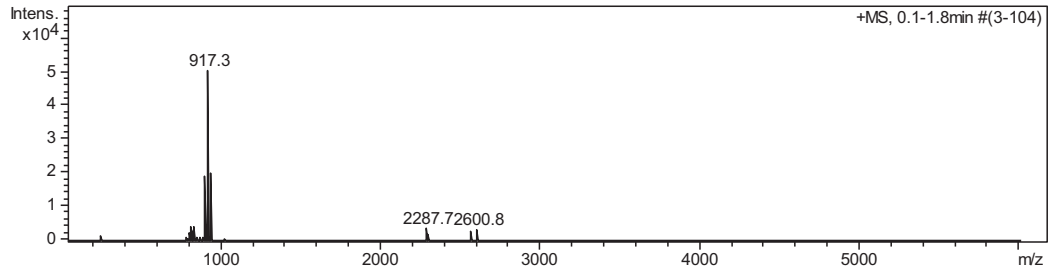

Reaction time: 70 h.

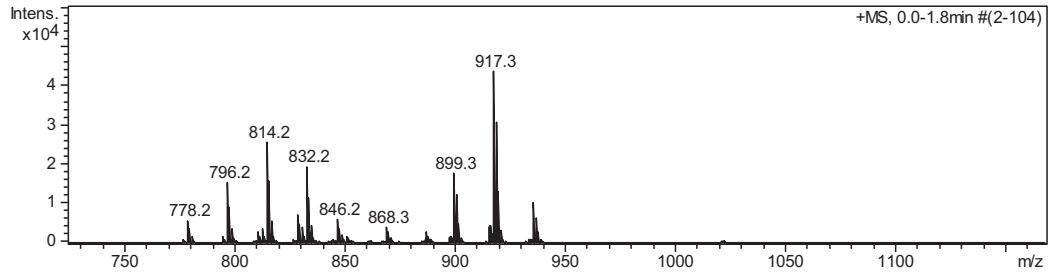

Fig. S2. Mass spectra recorded of the reaction mixture at times indicated.

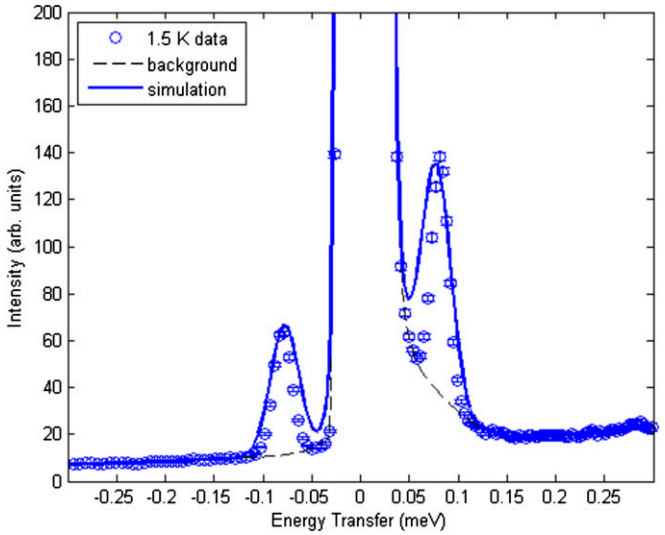

Fig. S3. Momentum-integrated energy spectra measured with a 9.0-Å setting at 1.5 K (blue open circles) on compound **3**. The inelastic intensity at 0.08 meV shows the zero field splitting of the S = 3/2 ground state quartet. The spin Hamiltonian simulation is represented by the blue solid line.

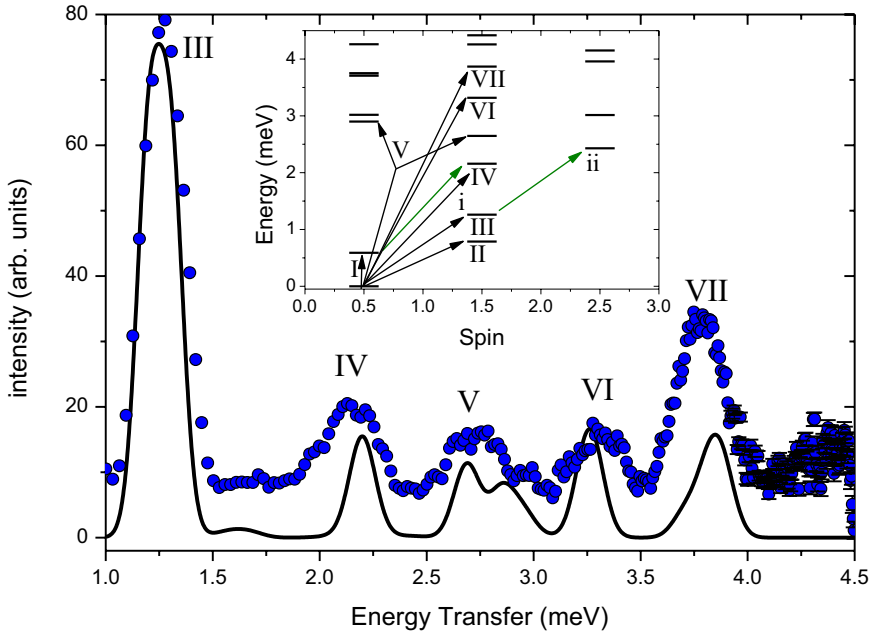

Fig. S4. Background subtracted INS energy spectrum with a 3.8-Å instrument setting measured at 1.5 K on sample **4** (blue filled circles). A simulation based on Hamiltonian (Eq. **1**) is represented by a solid blue line. (*Inset*) Calculated total spin eigenvalues for the isotropic part of Eq. **1**. Arrows and labels identify the excitations reached by the INS measurements.

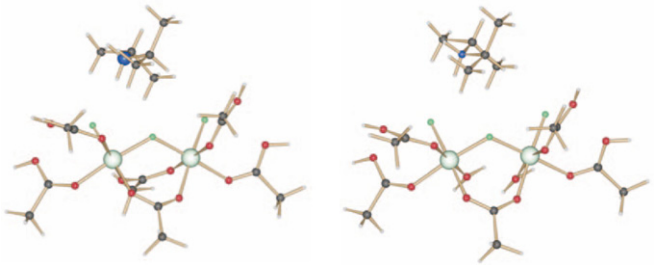

Fig. S5. Two models used to study the influence of loss of a carboxylate group from a Cr. . .Cr edge.